Sonoluminescence from a Single Bubble Driven at 1 Megahertz

Carlos Camara, Seth Putterman, and Emil Kirilov
Physics Department, UCLA, Los Angeles, California 90095, USA
(Received 18 November 2003; published 25 March 2004)

Measurements of the spectrum of sonoluminescence from an isolated bubble driven at 1 MHz are well fit by assuming thermal bremsstrahlung from a transparent 10^6 degree plasma. According to this interpretation, the photon-matter mean free path is larger than the light-emitting radius of a 1 MHz bubble, but smaller than the light-emitting radius for bubbles driven at ~40 kHz, thus accounting for the observed blackbody spectrum at 40 kHz.

DOI: 10.1103/PhysRevLett.92.124301 PACS numbers: 78.60.Mq

Sonoluminescence, an energy focusing process where sound is transduced into light by the pulsations of a gas bubble, can be observed over a remarkably large parameter space [1–7]. Theories have interpreted the spectrum of sonoluminescence (SL) as originating from thermal bremsstrahlung radiation from a weakly ionized plasma that forms in the highly compressed gas that is trapped inside a collapsing bubble [8–12]. In the most controlled realization of SL, the flashes of light are emitted from an isolated single bubble in water that is driven at acoustic frequencies ranging from 10 to 50 KHz [13–15]. The spectrum of light from these bubbles is best fit by an ideal Planck blackbody spectrum [16]. In fact, Planck's formula supplemented with the measured flash width Δt_{SL}, best-fit temperature T_e, and radius of light-emitting region R_e, gives the observed spectral irradiance within experimental accuracy for all noble gas (and hydrogen) bubbles. Furthermore, scaling laws exist which unify T_e and R_e for noble gas bubbles driven near the maximum acoustic pressures at which SL can be attained [17].

Interpreting SL in terms of Planck's law leads to small values of R_e. For helium and xenon bubbles oscillating at 40 kHz, R_e is about 100 and 400 nm, respectively. For the temperatures obtained by matching the spectra to blackbody curves (8000 K for Xe and 20 000 K for He) the values of R_e above are much smaller than the corresponding photon-matter mean free path l [18,19]. However, a key criterion for the attainment of a blackbody spectrum is that

$$R_e > l. \tag{1}$$

Since a blackbody is opaque, the measured temperature applies only to its surface. Could the interior be so hot that it is characterized by an l small enough that (1) is obeyed? To probe this possibility we study SL from smaller bubbles with the goal of reducing R_e to the point where the emitting region becomes transparent. Smaller bubbles are realized at higher acoustic frequencies [6], and so here we report measurements of a single sonoluminescing bubble driven at 1 MHz. Its spectrum (see Fig. 1) is no longer matched by Planck's law but instead is better fit to thermal bremsstrahlung from a transparent plasma with a temperature exceeding 500 000 K. According to these data it is possible to rationalize the blackbody spectrum of ~30 kHz bubbles by assuming an interior temperature that is much higher than the surface temperature, so that (1) can be realized in the interior.

The 1 MHz sound field was excited by piezoelectric ceramics housed inside brass end caps [Fig. 1 inset (Sonic

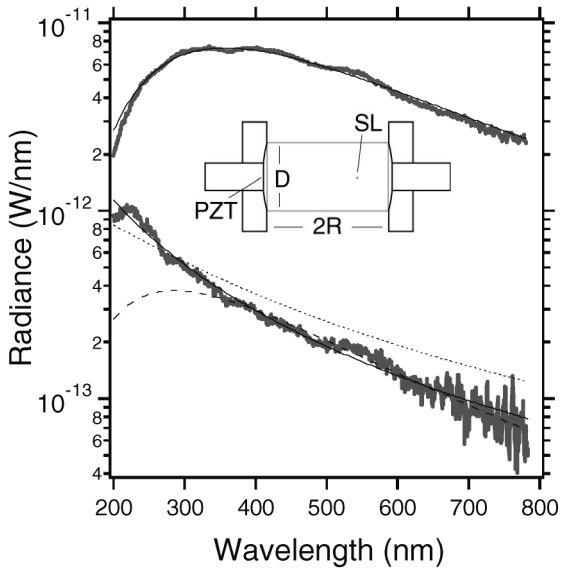

FIG. 1. Spectrum of single bubble sonoluminescence. Top trace (data) is for a bubble driven at 42 kHz in water with 3 Torr of dissolved xenon, taken with a resolution of 12 nm FWHM. These data are fit to blackbody radiation with a temperature of 8000° (top thin line). Bottom trace (data) is for a bubble driven at 1 MHz in water with 600 Torr of dissolved xenon, with a resolution of 70 nm FWHM. The solid line is a fit to bremsstrahlung radiation, with a temperature of 1×10^6 deg. The fine dashed line is also bremsstrahlung but with a temperature of 65 000°. The thick dashed line is blackbody radiation with a temperature of 10 000°. The inset is a diagram of the 1 MHz resonator used to generate and trap single bubbles. It consists of two thin ceramic transducers (PZTs) housed inside brass reflectors with a radius of curvature $R = 2.125$ in. The water was contained in a quartz cylinder of diameter $D = 3.1$ in between the reflectors.

Concepts, Woodinville, Washington)]. Insonated water was contained within a cylindrical quartz wall (outer diameter 3.1 in.) as shown. The radius of curvature of the end caps was matched to the length of the resonant region. At a high acoustic drive (typically in the range of 4–5 atm dynamic sound field pressure) light-emitting bubbles could be seen throughout the resonator. For a water-xenon mixture the emission is easily seen even with background lighting. By adjusting the amplitude and frequency of the drive, multibubble clouds could be suppressed and SL could be coaxed to appear from well-isolated bubbles.

A spectrum (Fig. 1) for a single SL bubble in water with xenon dissolved at a partial pressure of 600 Torr was obtained by collecting a portion of the emitted light with an imaging spectrometer (Acton research 300i with Princeton Instruments intensified CCD). The spectrum was acquired in three segments each of which spans 300 nm, allowing for an overlap of 100 nm between segments. The resolution is about 70 nm, and the background level was subtracted without gating but with the image intensifier in operation.

Two microchannel-plate photomultiplier tubes with transit-time spreads of about 25 ps were used to determine the flash width of the 1 MHz bubbles using time-correlated single photon counting [20,21]. Figure 2 shows the calibration curve for the system(taken with a femtosecond laser source pulsing at 1 kHz) along with the distribution of start-to-stop times (start and stop are determined by the recording of a photon in the Hamamatsu 3809U and 2809U photo detectors) for the 1 MHz bubble and a single bubble driven at 40 kHz. The deconvolved flash width Δt_{SL} of the 1 MHz single bubble is 98 ps, whereas the deconvolved width of the 40 KHz single bubble (300 Torr Xe in water) is 294 ps. A comparison of the single and coincidence count rates indicates that the sonoluminescing bubble is flashing one-third of the time during a 100 s run. From the "on" time and the spectrum we determine that each flash contains about 1000 photons.

As in prior studies the radius of the bubble as a function of time, "$R(t)$" was obtained by light scattering [22]. An 80 mW laser operating at 532 nm was used to illuminate the bubble. The actual light intensity to reach the bubble was 30 mW, which was focused to a spot size determined in air to be about 30 μm. The scattered light was collected by a 2 in. lens. Between the lens and the photomultiplier tube (PMT) were situated an aperture and neutral density filter ($\times 1/100$). The collected light spanned an angle ranging from 40° to 80° about the forward direction. Raw data displaying a single shot trace of light scattering along with SL are shown in Fig. 3, and the square root of the data with the background subtracted is shown in Fig. 4, where it is compared to a solution of the Rayleigh-Plesset (RP) equation of bubble motion [22]. For the range of angles over which light is collected the Mie scattering is proportional to the square of the radius down to about 0.8 μm [23,24]. Therefore, the curve plotted in Fig. 4 is proportional to the bubble radius. The constant of proportionality is determined from the fit to

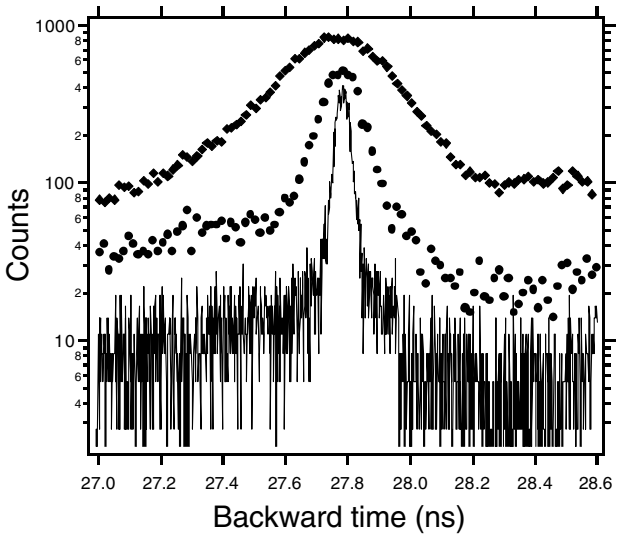

FIG. 2. Flash width of a single sonoluminescing xenon bubble in water taken with time-correlated single photon counting (TCSPC). The solid trace is a calibration obtained with 80 fs blue laser pulses. Circles are from a bubble in water with 600 Torr dissolved xenon, driven at 1 MHz. For the purpose of deconvolution data are fit to a Gaussian curve. The resulting FWHM is then 98 ps for the 1 MHz bubble and 294 ps for a single bubble formed from a 300 Torr solution of xenon in water driven at 40 kHz (square data).

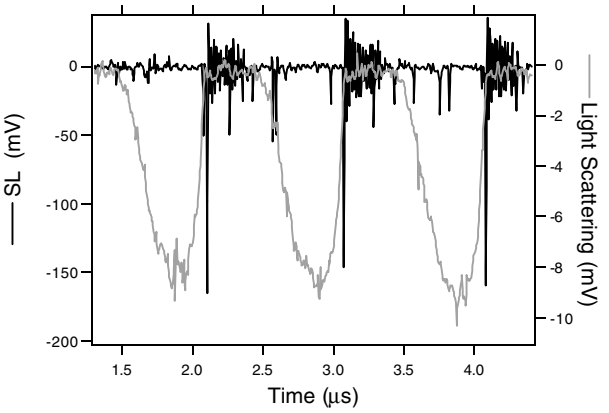

FIG. 3. Light scattering from a single SL bubble at 1 MHz.. Raw unaveraged data of light scattering (right axis) and light emission (left axis), taken with a photomultiplier tube (Hamamatsu R2027). The light scattering is taken with a low gain (−600 V) and through a neutral density 1/100 filter (ND2) to avoid saturating the PMT. The SL is taken for the same bubble by blocking the laser and removing the ND2 filter and increasing the gain to its maximum (−1200 V). All traces are timed relative to a fixed phase of the drive (Wavetek 186). The SL signals generate about two photoelectrons.

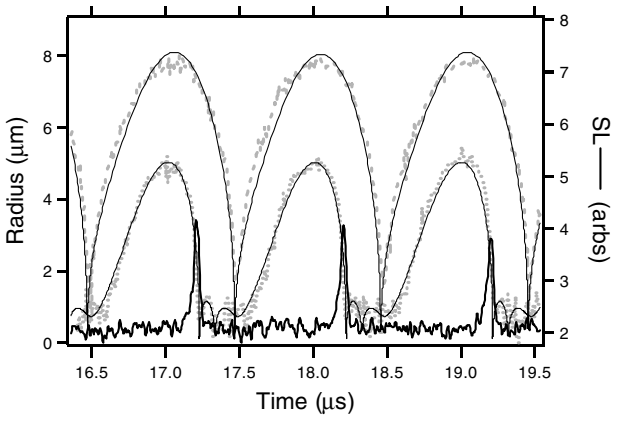

FIG. 4. Radius versus time for bubbles driven at 1 MHz in water with 550 Torr dissolved xenon. The smaller bubble (fine dotted line) is shown to be coincident with the light emission (right axis). The SL signal is an average over many cycles. This bubble is fit by a simulation of the RP equation of bubble dynamics with $R_0 = 0.8$ μm and Pa = 4 atm. The maximum velocity of bubble collapse obtained from the simulation is 2500 m/s. The single light-emitting bubbles were always accompanied by a larger bubble 100 μm away, shown as the thick dashed trace. This bubble is fit by an RP simulation with $R_0 = 2$ μm and Pa = 3 atm, which gives a maximum velocity of bubble collapse of 480 m/s.

the RP equation, which yields a maximum radius R_m of 5 μm and an ambient radius R_0 of 0.8 μm. Measuring the sound field using a needle hydrophone yields a peak amplitude of 4 atm which was used for this fit to the RP equation. The minimum or collapse radius R_c is beyond the sensitivity of this experiment. Assuming that the bubble collapses to its van der Waals hard core [15] R_c is ~100 nm. These steady-state values of the bubble radius are similar to values of R measured in transient situations [6].

Figure 4 also shows a second non-light-emitting bubble located 100 μm away from the SL bubble. This binary bubble system is a general feature of these 1 MHz experiments. Measurements of both bubbles were taken at the same gain so the relative light scattering intensities determine the ratio of maximum radii. The pressure used for the RP fit is now 3 atm because the distance between bubbles is about one-quarter of the distance from the pressure antinode to the pressure node.

An independent estimate of R_m can be obtained from a measurement of the fraction of laser light scattered by the bubble. The bubble is illuminated by 30 mW of light with a beam area $A_0 = 7 \times 10^{-6}$ cm^2. This corresponds to a flux N of 8.4×10^{10} laser photons per acoustic cycle. The maximum of R^2 is achieved for about one-seventh of a cycle so that the total number of photons/cycle to be scattered by the bubble and collected by the lens is $N_s = NK\pi R_m^2 \eta^2 / 7A_0$, where $K = 1.12 \times 10^{-2}$ is the cross-section factor for the ray limit [25] and $\eta \sim 0.87$ is the Fresnel factor. During this time, the PMT reads 9.0 mV above the noise. At the gain used (600 V on the Hamamatsu 2027) a single photoelectron registers an area of 2.5×10^{-13} V s. Using a quantum efficiency of 15% and correcting for the effects of a $\times 1/100$ neutral density filter imply that 3.6×10^6 photons are scattered towards the photodector during the time that R is near R_m. Equating these values of N_s yields $R_m \sim 3$ μm.

The photon-matter mean free path l arising from inverse bremsstrahlung is given in cgs units as [18,19]

$$1/l \sim 3.7 \times 10^8 (1 - e^{-h\nu/kT}) Z^3 n_c^2 / \nu^3 \sqrt{T}, \qquad (2)$$

where ν is the frequency of the light and T is the temperature in degrees Kelvin. The number of atoms of xenon per cc at ambient conditions follows from the ideal gas equation of state and is 2.4×10^{19} Xe/cc. So for a bubble with $R = 0.8$ μm, the number of gas molecules is 5×10^7. At the moment of collapse the particles are crushed to their van der Waals hard core yielding a density $n_c \sim 1.1 \times 10^{22}$ Xe/cc. For a temperature of 500 000 K we estimate the degree of ionization as being $Z \sim 4$, so that $n_+ \sim Z n_c$. For a wavelength $\lambda \sim 400$ nm ($\nu \sim 7.5 \times 10^{14}$ Hz) in the middle of the measured spectrum, which runs from 200–800 nm, one finds $l \sim 12$ nm. This mean free path is smaller than the radii of emission of the 40 kHz bubbles. Thus, if the interior of those bubbles is much hotter than the surface, then transport phenomena that are consistent with blackbody radiation and obey Eq. (1) could be supported.

The radius of emission of the putative thermal bremsstrahlung process that matches Fig. 1 can be estimated by considering the theoretically predicted value of the energy spectrum of a single flash:

$$\frac{dE}{d\lambda} = \frac{16\pi^2 e^6 Z^3 n_c^2}{\sqrt{3kT} m_e^{3/2} c^2 \lambda^2} e^{-hc/\lambda kT} [4\pi R_e^3 \Delta t_{\mathrm{SL}}/3], \qquad (3)$$

where c is the speed of light. Applying this expression to the experimental fits, one finds that $R_e \sim 2$ nm, which is small compared to l, and accounts self-consistently for the interpretation of the spectrum at 1 MHz as originating in a transparent medium.

The total thermal energy E_T in a region at 1×10^6 K can be substantially greater than the amount of radiated light. So here we compare E_T to the potential energy V_B stored in the bubble at its maximum radius,

$$\frac{E_T}{V_B} \approx \frac{R_e^3 n_c Z k T_e}{R_m^3 p_0},$$

and find that the thermal energy is down from the available mechanical energy by 3 orders of magnitude. Furthermore, the thermal energy is about 30 times the energy of the radiated light (200–800 nm).

The observed ambient and maximum radii of the bubble are consistent with measurements on cavitating clouds driven at the same frequency [6]. The 1×10^6 K temperature provides a picture of how the 30–40 kHz

bubbles could be blackbodies in spite of their submicron size. Most mysterious is the nanometer size for the region of emission as determined by a match of the spectrum to thermal bremsstrahlung from an ionized plasma. On the one hand, it is a challenge to understand how an acoustic signal with a wavelength of 1 mm focuses its energy to an atomistic dimension. On the other hand, molecular dynamic simulations of a xenon bubble with about 1×10^6 (xenon) hard spheres do display spatial structure on the scale of the collapsed bubble radius divided by 20. In addition, depending on the boundary conditions, the interior of these bubbles can reach $Z = 4$ and temperatures over 100 000 K [26]. It remains to be seen if such short length scales characterize simulations with $N_0 \sim 5 \times 10^7$ particles as would be appropriate for the 1 MHz bubble.

For temperatures of 500 000 K the thermal velocity of the electrons is about 5×10^8 cm/s, and the hot spot plasma frequency is $\omega_p/2\pi = 2 \times 10^{15}$ Hz. We then find that $Zn_c[v_{th}/\omega_p]^3 \approx 2.5$. The extent to which this quantity is much bigger than 1 is the extent to which one is dealing with a hot plasma and the various formulas (e.g., bremsstrahlung) apply [27].

The parameter space for sonoluminescence from an isolated bubble has been extended to acoustic driving frequencies of 1 MHz. The ambient radii are about a factor of 5 smaller than for bubbles driven at 30 kHz, and the spectra are significantly more ultraviolet. If the light is due to a thermal source, then its temperature is above 10^5 K. This interpretation suggests that the blackbody spectra of larger bubbles, like the 30 kHz ones, can be explained in terms of a hot interior which allows for a photon-matter mean free path smaller than R_e.The radius of emission resulting from the bremsstrahlung fit is so small as to beg for an independent measurement.

We thank Alex Bass for valuable assistance with analysis of the Mie scattering, and Brian Naranjo and Keith Weninger for valuable advice regarding many aspects of this work. Support from the U.S. DOE Division of Materials Science and Engineering and DARPA is gratefully acknowledged.

[1] A. J. Walton and G. T. Reynolds, Adv. Phys. **33**, 595 (1984).
[2] S. Putterman and K. Weninger, Annu. Rev. Fluid Mech. **32**, 445 (2000).
[3] K. R. Weninger, C. G. Camara, and S. J. Putterman, Phys. Rev. Lett. **83**, 2081 (1999).
[4] C. K. Su, C. Camara, B. Kappus, and S. J. Putterman, Phys. Fluids **15**, 1457 (2003).
[5] E. B. Flint and K. Suslick, Science **253**, 1397 (1991).
[6] K. R. Weninger, C. G. Camara, and S. J. Putterman, Phys. Rev. E **63**, 016310 (2000).
[7] Y. Didenko and K. S. Suslick, Nature (London) **418**, 394 (2002).
[8] C. C. Wu and P. H. Roberts, Phys. Rev. Lett. **70**, 3424 (1993).
[9] S. Hilgenfledt, S. Grossman, and D. Lohse, Nature (London) **398**, 402 (1999).
[10] S. Putterman, P. G. Evans, G. Vazquez, and K. Weninger, Nature (London) **409**, 782 (2001).
[11] M. P. Brenner, S. Hilgenfeldt, and D. Lohse, Rev. Mod. Phys. **74**, 425 (2002).
[12] T. K. Saksena and W. L. Nyborg, J. Chem. Phys. **53**, 1722 (1970).
[13] P. R. Temple, MS thesis, University of Vermont, 1970.
[14] D. F Gaitan, L. A. Crum, C. C. Church, and R. A. Roy, J. Acoust. Soc. Am. **91**, 3166 (1992).
[15] B. P. Barber and S. J. Putterman, Nature (London) **352**, 318 (1991).
[16] G. Vazquez, C. Camara, S. Putterman, and K. Weninger, Opt. Lett. **26**, 575 (2001).
[17] G. Vazquez, C. Camara, S. J. Putterman, and K. Weninger, Phys. Rev. Lett. **88**, 197402 (2002).
[18] S. Glasstone and R. H. Loveberg, *Controlled Thermonuclear Reactions* (Van Nostrand, New York, 1960); L. Spitzer, *Physics of Fully Ionized Gases* (Interscience, New York, 1956).
[19] Ya B. Zeldovich and Yu P. Raizer, *Physics of Shock Waves and High Temperature Hydrodynamic Phenomena* (Academic, New York, 1966).
[20] B.Gompf, R. Gunther, G. Nick, R. Pecha, and W. Eisenmenger, Phys. Rev. Lett. **79**, 1405 (1997).
[21] R. A. Hiller, S. J. Putterman, and K. R. Weninger, Phys. Rev. Lett. **80**, 1090 (1998).
[22] B. P. Barber, R. A. Hiller, R. Lofstedt, S. J. Putterman, and K. R. Weninger, Phys. Rep. **281**, 65 (1997).
[23] K. R. Weninger, P. G. Evans, and S. J. Putterman, Phys. Rev. E **61**, 1020 (2000).
[24] K. R. Weninger, P. G. Evans, and S. J. Putterman, Phys. Rev. E **64**, 038301 (2001).
[25] G. E. Davis, J. Opt. Soc. Am. **45**, 572 (1955).
[26] S. J. Ruuth, S. Putterman, and B. Merriman, Phys. Rev. E **66**, 036310 (2002).
[27] J. F. Benage, W. R. Shanahan, E. G. Sherwood, L. A. Jones, and R. J. Trainor, Phys. Rev. E **49**, 4391 (1994); M. A. Berkovsky, D. Kelleher, Yu K. Kurilenkov, M. Skowronek, J. Phys. B **26**, 2475 (1993).